

1 Article

2 Surface Response Methodology-Based Mixture 3 Design to Study the Influence of Polyol Blend 4 Composition on Polyurethanes Properties

5 Said Arévalo-Alquichire^{1,2}, Maria Morales-Gonzalez¹, Luis Diaz³ and Manuel Valero^{1,*}6 ¹ Energy, materials and environment group, faculty of engineering, Universidad de La Sabana, Chia,
7 Colombia8 ² Doctoral program of biosciences, Universidad de La Sabana, Chia, Colombia9 ³ Bioprospecting research group, faculty of engineering, Universidad de La Sabana, Chia, Colombia

10 * Correspondence: manuelvv@unisabana.edu.co; Tel.: +57 1 8615555 x 25224

11

12 Abstract: Polyurethanes are materials with a strong structure-property relationship. The goal of this
13 research was to study the effect of a polyol blend composition of polyurethanes on its properties
14 using a mixture design and setting mathematic models for each property. Water absorption,
15 hydrolytic degradation, contact angle, tensile stretch, hardness and modulus were studied.
16 Additionally, Thermal stability was studied by thermogravimetric analysis. Area under the curve
17 was used to evaluate the effect of polyol blend composition on thermal stability and kinetics of water
18 absorption and hydrolytic degradation. Least squares were used to calculate the regression
19 coefficients. Models for the properties were significant, and lack of fit was not ($P < 0.05$). Fit statistics
20 suggest both good fitting and prediction. Water absorption, hydrolytic degradation and contact
21 angle were mediated by the hydrophilic nature of the polyols. Tensile strength, modulus and
22 hardness could be regulated by the molecular weight and hydroxyl index of the polyols. Regression
23 of DTG curves from thermal analysis showed improvement of thermal stability with the increase of
24 PCL and PE. An ANOVA test of the model terms demonstrated that three component effects on
25 bulk properties like water absorption, hydrolytic degradation, hardness, tensile strength and
26 modulus, and the PEG*PCL interaction with the contact angle, which is a surface property. Mixture
27 design application allowed for an understanding of the structure-property relationship through
28 mathematic models.

29 **Keywords:** polyurethane; polyol; Mixture design; Design of experiment; structure-properties
30 relationship
31

32 1. Introduction

33 Polyurethanes (PUs) are a special group of polymers with a wide range of applications in
34 industry, including in adhesives, aircrafts, furniture, isolation, construction and biomedical
35 applications. Versatility is explained by the variety of properties expressed by PUs, which are closely
36 related with its composition[1]. The primary synthesis begins with the reaction of a poly-hydroxyl
37 donor called a polyol and isocyanate to form a urethane bond. The structure depends on the ratios of
38 the compounds. PUs can be obtained in flexible and rigid foams, thermoplastics, coatings, adhesives,
39 sealants, elastomers, waterborne dispersions[2] and hydrogels[3]. The three main components in
40 polyurethane synthesis are the polyol, isocyanate and chain extenders or crosslinkers. Polyols form
41 the soft segment, and isocyanate and a chain extender or crosslinker form the hard segment. The
42 nature of the polyol and the hard segment content in PUs could regulate both bulk and surface
43 properties[1].
44

45 Thus, studies of polyol composition have been carried out. Trzebiatowska et al. (2018) obtained
46 polyurethanes from the glycerolysate of recycled polyurethanes and poly(ethylene-butylene) adipate
47 diol. As the content of the recycled component increased, the swelling ratio decreased, and the
48 crosslink density simultaneously increased, resulting in the rise of glass transition and storage
49 modulus at room temperature. Thermomechanical stability, tensile strength, elastic modulus and
50 hardness of the PUs also increased and elongation at break decreased with the incorporation of
51 glycerolysate. The original polyol used was tri-functional, and as such, it is possible to have more
52 linkages per polyol molecule. Additionally, more networks could be created in this material as its
53 structure is more branched. These properties can result in a reduction in polymer chains
54 movement[2].

55
56 Bil et al. (2010) worked with aliphatic poly(ester-urethanes) from poly(ϵ -caprolactone) diol having
57 different molecular masses ($M = \sim 530, 1250$ and 2000 Da), cycloaliphatic diisocyanate 4,4'-
58 methylenebis (cyclohexyl isocyanate) and ethylene glycol as a chain extender. Changes in the
59 macromolecule order, with increasing hard segment content, were observed via modulated
60 differential scanning calorimetry. Depending on the hard segment content, gradual variations in the
61 polyurethane surface properties were observed. Furthermore, as the content of the hard segments
62 increased, the polyurethane surface exhibited more phase separation, a higher content of urethane
63 moieties and higher hydrophilicity[4]. Moreover, previous work in our lab has been focused on the
64 effect of polyol as well. Uscategui et al. (2017) evaluated the effects of the type of polyols, derived
65 from castor oil by transesterification with pentaerythritol, with the incorporation of low
66 concentrations of chitosan on the mechanical and biological properties of the polymer. The goal of
67 this study was to obtain suitable materials in the design of biomaterials showing that increasing
68 physical crosslinking increased the mechanical and adhesive properties, and bacterial inhibition
69 depended on the polyol and percentage of chitosan[5].

70
71 Additionally, chain extenders and crosslinkers could tune the mechanical properties and hydrolytic
72 stability of PUs. They are low molecular weight compounds that produce elastomeric behavior in
73 PUs. Difunctional molecules are considered chain extenders, and higher functionalities are classified
74 as crosslinkers. Shoaib et al. (2018) studied the effect of amino acid incorporation as chain extenders
75 on the biocompatible and biodegradable properties, and pH responsive drug delivery of
76 polyethylene glycol-based PUs. All PUs showed higher swelling ability (4–13%), hydrolytic
77 degradation (20–38%) and cell viability (>90%). Additionally, arginine had lower values of release at
78 pH 7.4 as a chain extender, which resulted in less toxicity while fulfilling the requirements. However,
79 at lower pH, behavior change due to the presence of free amino groups in arginine, which were
80 protonated in the presence of acidic conditions, resulted in greater swelling and solvent penetration,
81 thus increasing drug release[6].

82
83 Most of those works reported valuable knowledge about the effects of polyols and chain extenders.
84 However, most qualitatively described the interactions between the components of the PUs based on
85 the performance of some properties or, in some cases, just analyzed the behavior of one parameter.
86 To establish the impact of these interactions quantitatively, design of experiment can be used. Design
87 of experiment is a well established concept for the planning and execution of informative
88 experiments[7]. Experimental design is a specific set of experiments defined by a matrix composed
89 by the different level combinations of the variables studied[8]. One type of design applications
90 concerns the preparation and modification of mixtures. This involves the use of mixture designs to
91 explore the effect on mixture properties[7]. Experimental design has advantages such as cost and time
92 economy, a reduced number of runs required to analyze the effects and the analysis of more than one
93 factor at a time[9]. In the polymer field, Olivato et al. (2013) proposed a mixture model to evaluate
94 the effect of tartaric acid on the properties of starch/poly(butylene adipate co-terephthalate) blown
95 films plasticized with glycerol. They found that the interaction between the polymer and tartaric acid
96 has a positive effect on the tensile strength and puncture force. Additionally, a greater proportion of

97 tartaric acid increased Young's modulus and contributed to the reduction in water vapor
98 permeability[10]. Abolghasemi Fakhri et al. (2018) studied ternary-based nanocomposites based on
99 polystyrene, nanoclay and zinc oxide nanoparticles for food packaging material using a central
100 composite design-based response surface methodology. They found a synergistic effect between
101 nanoclay and zinc oxide, resulting in the improvement of the mechanical and color properties of the
102 mixture[11].

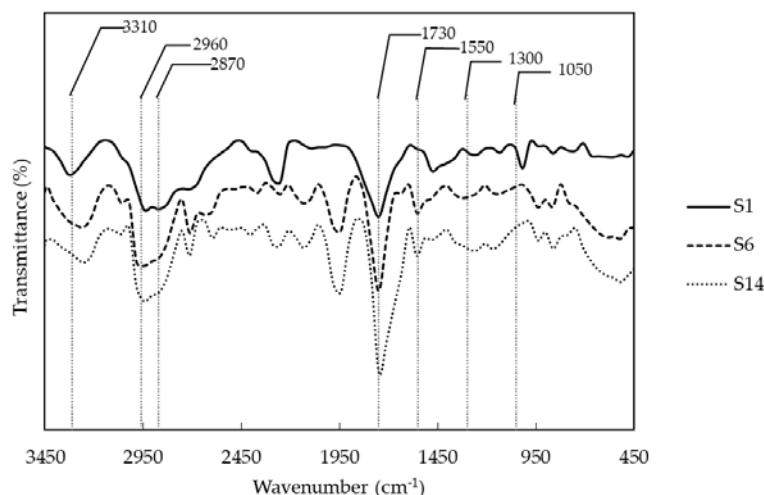
103
104 Specifically, in the polyurethanes field, Li et al. (2017) examined bio-based flexible polyurethane
105 foams using bio-polyol, extracted from the fast pyrolysis oil of wheat straw, foaming processes such
106 as the bio-polyol to petroleum-based polyol ratio, the polymethylene polyphenylene isocyanate to
107 polymeric diphenyl-methane diisocyanate ratio, and the crosslinking agent content was optimized
108 using response surface methodology. Resilience was found to increase with an increasing amount of
109 petroleum-based polyol, while for bio-polyol, resilience was decreased up to a medium dosage after
110 which there was a slight increase. However, increasing the amount of polymethylene polyphenylene
111 isocyanate along with the petroleum-based polyol had a positive influence on the resilience of PUs,
112 though it declined at a high dosage of polymethylene polyphenylene isocyanate[12]. Zhao et al. (2018)
113 fabricated expanded thermoplastic polyurethane bead foams with supercritical CO₂ as a blowing
114 agent. They studied the influences of saturation pressure, temperature and soaking time and their
115 interactions on foaming behavior through a response surface methodology based on the Box-
116 Behnken design. This showed that saturation temperature was the most significant parameter
117 affecting the expansion ratio, shrinkage ratio, and cell morphology of PUs foams. There was an
118 interaction effect between saturation temperature and soaking time, wherein the expansion ratio of
119 the foams was more sensitive to changes in soaking time at higher temperatures. As the soaking time
120 increased, the shrinkage of PUs foams increased first and then leveled off, and the cell diameter
121 decreased significantly[13].

122
123 Despite interest in understanding the structure-property relationship of polyurethanes, to the best of
124 our knowledge there are no reports regarding the application of design of experiments to evaluate
125 the influence of monomer composition on polyurethanes. Thus, the goal of this research is to evaluate
126 the effect of polyol blend composition on the properties of polyurethanes, including water absorption,
127 hydrolytic degradation, contact angle, tensile strength and modulus, through mixture design and
128 data regression, generating mathematic models to better understand the structure-property
129 relationship in PUs.

130 2. Results & Discussion

131 2.1. Polyurethane synthesis and chemical structure

132 In this work, effect of polyol composition and crosslinker concentration was evaluated on different
133 properties like: thermal behavior, hydrophilicity and hydrolytic degradation and mechanical
134 behavior based on tensile test and hardness. Polyethylene glycol (PEG), Polycaprolactone diol (PCL)
135 and pentaerythritol (PE) concentrations were studied. From this point, polyol blend should be
136 understood as the combination of PEG, PCL and PE.



137

138 Figure 1. Representative infrared spectra of polyurethanes with different combination of polyols. S1)
 139 PCL and PE, S6) PCL, PEG and PE, and S14) PEG and PE

140

141 Successful of polyurethane synthesis was evaluated by FTIR (Fourier transform infrared
 142 spectroscopy). **Figure 1** shows the functional groups of some synthesized polyurethanes with
 143 different polyol combinations. In general, polymers show the following peaks: at approximately 3310
 144 cm^{-1} , we observed the overtone related with the stretching of N-H bond from urethane and, near
 145 1550 cm^{-1} , the original signal. The asymmetric and symmetric vibration signals of $-\text{CH}_2$ from the soft
 146 segments of the PCL and PEG and PE, from the hard segment, were observed at 2960 and 2870 cm^{-1} .
 147 At 1730 cm^{-1} , we can see the characteristic peak of urethane bond related with $-\text{C}=\text{O}$ stretching.
 148 Additionally, between 1300 and 1050 cm^{-1} , there are two peaks related to the asymmetric and
 149 symmetric stretching of $-\text{C}-\text{O}-\text{C}-$ group, which is also part of the urethane bond. Finally, under 1050
 150 cm^{-1} , there are peaks related to the vibration of the aliphatic ring from the IPDI. According to the
 151 above, polyurethanes were obtained with an integration of polyols, crosslinker and isocyanate
 152 structures.

153 2.2. Mixture design

154 In this work, we applied a mixture design to study the influence of polyol blend composition. It
 155 had 9 design points with 7 repetitions (See Table 4). Three of the design points were located at the
 156 extreme where PCL was the major component represented by S1, S2, S3, S4, S5. Another three points
 157 were in the middle of the experimental space (S6, S7, S8, S9, S10, S11). Finally, three points at the
 158 opposite extreme where PEG was the major component (S12, S13, S14, S15, S16).
 159

160 Responses were analyzed by box-cox distribution. Transformations were carried out according with
 161 box-cox suggestions. Therefore, the inverse square root of water absorption and the square root
 162 of hydrolytic degradation and tensile stretch were applied. Non-transformations were made on
 163 contact angle, modulus, hardness, kinetics of water absorption and hydrolytic degradation, and
 164 thermal responses. Additionally, DFFITS tests was applied to identify influential points. For
 165 contact angle, 2 influential points were deleted from the analysis (S15 and S16). Response of S11
 166 and S7 were removed for kinetics of water absorption and thermal response, respectively.
 167

168 Table 1. ANOVA test of model regression for water absorption, contact angle and hydrolytic degradation

Source	Water absorption						Contact angle					Hydrolytic degradation						
	SS	DF	MS	F	p-value		SS	DF	MS	F	P-value		SS	DF	MS	F	p-value	
Model	6.E-01	6	1.E-01	3.E+02	<0.0001	a	5.E+03	5	1.E+03	4.E+01	2.E-05	a	6.E+01	6	1.E+01	1.E+02	1.E-07	a
Linear Mixture	5.E-01	2	2.E-01	8.E+02	<0.0001	a	4.E+03	2	2.E+03	7.E+01	7.E-06	a	5.E+01	2	3.E+01	3.E+02	9.E-09	a
PEG*PCL	1.E-01	1	1.E-01	3.E+02	<0.0001	a	5.E+02	1	5.E+02	2.E+01	3.E-03	a	1.E+00	1	1.E+00	1.E+01	5.E-03	a
PEG*PE	3.E-04	1	3.E-04	8.E-01	4.E-01		1.E-01	1	1.E-01	6.E-03	9.E-01		1.E-01	1	1.E-01	1.E+00	3.E-01	
PCL*PE	3.E-04	1	3.E-04	8.E-01	4.E-01		2.E-02	1	2.E-02	8.E-04	1.E+00		9.E-02	1	9.E-02	9.E-01	4.E-01	
PEG*PCL*PE	7.E-03	1	7.E-03	2.E+01	1.E-03	a	-	-	-	-	-		5.E+00	1	5.E+00	5.E+01	6.E-05	a
Residual	3.E-03	9	3.E-04				2.E+02	8	3.E+01				9.E-01	9	1.E-01			
Lack of Fit	4.E-04	2	2.E-04	6.E-01	6.E-01	b	6.E+00	1	6.E+00	2.E-01	7.E-01	b	3.E-02	2	1.E-02	1.E-01	9.E-01	b
Pure Error	2.E-03	7	3.E-04				2.E+02	7	3.E+01				9.E-01	7	1.E-01			
Total	6.E-01	15					5.E+03	13					6.E+01	15				

169 a: Significant at the 95% level; b: Not significant at the 95% level; DF: Degrees of freedom; SS: Sum of squares; MS: Mean square; F: Ratio

170

171

172 Table 2. ANOVA test of model regression for thermal stability, water absorption kinetics and hydrolytic degradation kinetics

Source	Thermal Stability						Water absorption kinetics					Hydrolytic degradation kinetics						
	SS	DF	MS	F	p-value		SS	DF	MS	F	p-value		SS	DF	MS	F	p-value	
Model	6.E-01	2	3.E-01	9.E+01	4.E-08	a	2.E+08	6	3.E+07	2.E+03	5.E-12	a	3.E+07	6	6.E+06	3.E+02	6.E-10	a
Linear Mixture	6.E-01	2	3.E-01	9.E+01	4.E-08	a	1.E+08	2	5.E+07	3.E+03	2.E-12	a	3.E+07	2	2.E+07	9.E+02	5.E-11	a

PEG*PCL	-	-	-	-	-		6.E+06	1	6.E+06	4.E+02	4.E-08	a	3.E+06	1	3.E+06	1.E+02	8.E-07	a
PEG*PE	-	-	-	-	-		1.E+05	1	1.E+05	8.E+00	2.E-02		4.E+04	1	4.E+04	2.E+00	2.E-01	
PCL*PE	-	-	-	-	-		2.E+04	1	2.E+04	1.E+00	3.E-01		3.E+04	1	3.E+04	2.E+00	2.E-01	
PEG*PCL*PE	-	-	-	-	-		1.E+07	1	1.E+07	9.E+02	2.E-09		3.E+06	1	3.E+06	1.E+02	9.E-07	a
Residual	4.E-02	12	3.E-03				1.E+05	8	1.E+04				2.E+05	9	2.E+04			
Lack of Fit	2.E-02	6	4.E-03	1.E+00	5.E-01	b	4.E+04	2	2.E+04	1.E+00	3.E-01	b	3.E+04	2	1.E+04	8.E-01	5.E-01	b
Pure Error	2.E-02	6	3.E-03				8.E+04	6	1.E+04				1.E+05	7	2.E+04			
Total	7.E-01	14					2.E+08	14					3.E+07	15				

173 a: Significant at the 95% level; b: Not significant at the 95% level; DF: Degrees of freedom; SS: Sum of squares; MS: Mean square; F: Ratio

174

175 Table 3. ANOVA of model regression of tensile strength, modulus and hardness

Source	Tensile Strength						Modulus						Hardness					
	SS	DF	MS	F	p-value		SS	DF	MS	F	p-value		SS	DF	MS	F	p-value	
Model	6.E+00	6	9.E-01	4.E+01	4.E-06	a	0,0054	6	0,0009	289,06	<0.0001	a	2.E+03	6	4.E+02	5.E+01	2.E-06	a
Linear																		
Mixture	4.E+00	2	2.E+00	9.E+01	1.E-06	a	0,0040	2	0,0020	643,17	<0.0001	a	8.E+02	2	4.E+02	6.E+01	8.E-06	a
PEG*PCL	5.E-02	1	5.E-02	2.E+00	2.E-01		0,0001	1	0,0001	36,47	0,0002	a	2.E+01	1	2.E+01	3.E+00	1.E-01	
PEG*PE	2.E-02	1	2.E-02	1.E+00	3.E-01		1.E-03	1	1.E-03	0,4333	0,5268		4.E+00	1	4.E+00	6.E-01	5.E-01	
PCL*PE	2.E-02	1	2.E-02	7.E-01	4.E-01		6.E-05	1	6.E-05	0,0185	0,8949		4.E+00	1	4.E+00	6.E-01	5.E-01	
PEG*PCL*PE	5.E-01	1	5.E-01	2.E+01	1.E-03	b	0,0005	1	0,0005	145,77	<0.0001	a	1.E+03	1	1.E+03	1.E+02	1.E-06	a
Residual	2.E-01	9	2.E-02				0,0000	9	3.E-03				7.E+01	9	7.E+00			
Lack of Fit	5.E-02	2	3.E-02	1.E+00	4.E-01	b	3.E-03	2	2.E-03	0,4629	0,6474	b	2.E+01	2	1.E+01	2.E+00	2.E-01	b
Pure Error	1.E-01	7	2.E-02				0,0000	7	4.E-03				4.E+01	7	6.E+00			
Total	6.E+00	15					0,0054	15					2.E+03	15				

176 a: Significant at the 95% level; b: Not significant at the 95% level; DF: Degrees of freedom; SS: Sum of squares; MS: Mean square; F: Ratio

177

178

179

180 Special cubic models were fit for each response for the regression models. Model regression based on
 181 the least square was used to compute the coefficients. The equations are presented in Table 2. Models
 182 were evaluated by ANOVA.

183

Table 4. Equations representing the models for the five properties studied

Property	Units	Model Equation
Thermal Stability (Th)	1/°C	$Th = 5.134*PEG + 5.700*PCL + 4.707*PE$
Water Absorption (WA)	%	$1/\sqrt{WA} = 0.047*PEG + 0.534*PCL + 7.872*PE - 0.101*PEG * PCL - 7.233*PEG * PE - 6.928*PCL * PE - 10.499*PEG * PCL * PE$
Contact Angle (CA)	Degrees	$CA = 2.09*PEG + 110.073*PCL + 220.13*PE - 75.353*PEG * PCL + 469.808*PEG * PE - 182.699*PCL * PE$ $\sqrt{Deg} = -1.077*PEG - 3.884*PCL - 455.857*PE +$
Hydrolytic degradation (Deg)	%	$23.734*PEG * PCL + 585.13*PEG * PE + 557.423*PCL * PE - 278.709*PEG * PCL * PE$
Water Absorption kinetics (KWA)	S	$KWA = 28562.969*PEG + 3753.102*PCL + 530986.252*PE - 43858.222*PEG * PCL - 835976.018*PEG * PE - 624450.94*PCL * PE + 523435.575*PEG * PCL * PE$
Hydrolytic degradation kinetics (Kdeg)	S	$Kdeg = -525.686*PEG - 2362.406*PCL - 300106.634*PE + 14011.812*PEG * PCL + 383372.797*PEG * PE + 358429.093*PCL * PE - 197168.276*PEG * PCL * PE$ $\sqrt{TS} = 0.899*PEG - 0.123*PCL + 77.941*PE + 7.793*PEG * PCL - 86.277*PEG * PE - 55.399*PCL * PE - 85.572*PEG * PCL * PE$
Tensile stretch (TS)	Mpa	
Modulus (E)	MPa	$E = -0.012*PEG - 0.043*PCL - 0.912*PE + 0.228*PEG * PCL + 1.184*PEG * PE + 2.145*PCL * PE - 2.659*PEG * PCL * PE$
Hardness (HD)	Shore A	$HD = -21.324*PEG + 0.643*PCL - 4231.919*PE + 372.187*PEG * PCL + 5662.460*PEG * PE + 5682.430*PCL * PE - 3878.500*PEG * PCL * PE$

184

185 The ANOVA test for the fitted models (see Table 1, Table 2 and Table 3) demonstrated that the model
 186 sum of squares was statistically significant at a 95% probability level (P-value < 0.05) for the five
 187 properties studied. In addition, lack of fit was not significant at a 95% probability level (P-value >
 188 0.05) in all cases. Both, the model sum of square and lack of fit indicated that the models were
 189 adequate. Likewise, fit statistics confirmed good fitting for all properties. According with Olivato,
 190 J.B. et al. (2013), an R-square value higher than 0.7 suggests a good fit with the experimental data[10].
 191 In this study, all R-square values were over 0.96. Additionally, the adjusted R-square value was
 192 calculated to be greater than 0.94, demonstrating that the variations in the responses can be explained
 193 by the relationships obtained. In the same way, the predicted R-square value determined how well
 194 the model predicts response. Here, the values were over 0.8. Therefore, the models obtained herein
 195 are promising for the evaluation of the structure-property relationship of polyurethanes.

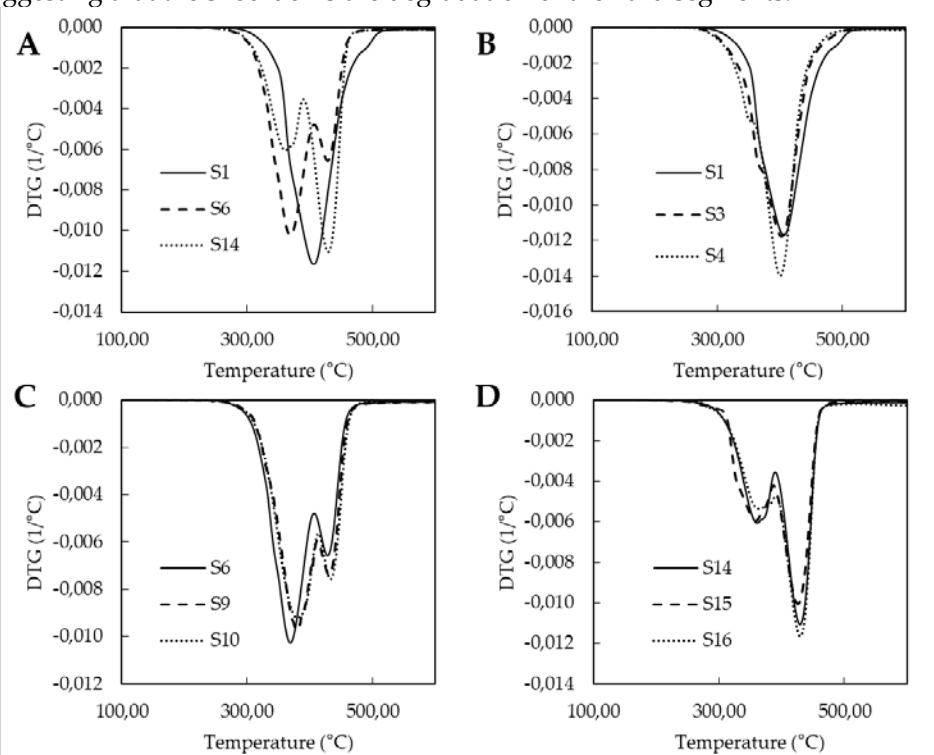
196

2.3. Thermal behavior

197 Thermal analysis was carried out by thermogravimetric analysis (TGA). Curves were
 198 normalized with respect to initial sample weight. First derivate was calculated for each sample.
 199 Figure 2 shows the thermal degradation of some polymers from different mixtures. According with
 200 Sui et. al. (2013) polyurethanes degrade in three steps starting with the hard segments between 250
 201 to 320 °C, following by two components produced after the cleavage of the urethane linkages. First
 202 the smaller molecular weight compounds linked to urethane bond like the crosslinker and second,
 203 the soft segment chains [14].

204

205 Figure 2A, compare the behavior of samples from the extremes and middle of the experimental
 206 design. S1 seems to describe one degradation stage, while S6 and S14 shows two stages. S16 shows
 207 and increase on second stage compared with S6. Studying the curves from the PCL extreme points
 208 (Figure 2B), they present a shoulder around 350°C. S1 have the largest amount of PE which produce
 209 PUs with large amount of hard segment. This could produce an overlapping of the three stages due
 210 to the large amount of PUs pyrolysis. S3 and S4 have lower levels of PE and they show better defined
 211 shoulders suggesting that the shoulder is the degradation of the hard segments.



212

213 Figure 2. Derivate thermogravimetric curves for different polyol blend combinations A) Comparison
 214 of DTGs from the extremes and middle design points. B) DTGs of PCL extreme design points, C)
 215 DTGs of middle design points and D) PEG extreme design points.

216 By other hand, Figure 2C shows the behavior of the samples from the middle design points. Here,
 217 two separate stages could be identified. First one associated to the hard segment degradation and the
 218 second over the 400°C with the soft segment. Figure 2D showed the behavior of the PEG extreme
 219 points. The same two stages could be observed, however second stages had largest area under the
 220 curve than curves in Figure 2C, it could suggest that higher amount of hard segment was produced
 221 in the middle points than the PEG extreme points. Additionally, related the crosslinking density with
 222 the thermal stability and PCL extreme points present the highest content of hard segment.

223

224 About the onset temperatures (Table 5), PUs were thermally stable under 220°C. Polymers with
 225 higher amount of PE showed higher values. Additionally, polymers with higher concentrations of
 226 PCL had higher temperatures. The addition of PEG reduced the onset temperatures. Król et. al. (2007)
 227 described that polyesterurethanes are more stable thermally than polyetherurethanes; ester bonds

228 undergo decomposition within 390 to 440°C while ether decompose between 360-400 °C [15]. Our
 229 finding confirms that behavior, PCL is a polyester and the PCL extreme points described the higher
 230 values of onset temperature.

231 Table 5. Onset temperatures of PUs synthesized

Sample	Onset Temperature (°C)
S1	273.21
S2	276.84
S3	264.15
S4	263.92
S5	274.08
S6	262.17
S7	254.05
S8	268.65
S9	260.56
S10	253.74
S11	258.31
S12	264.82
S13	262.20
S14	261.75
S15	225.60
S16	263.08

232 To study the effect of composition, regression of onset temperatures was carried out. However, poor
 233 fitting properties were obtained (R-square = 0.64). So, the absolute normalized area under the curve
 234 (nAUC) of the DTG curves were fitted as approach to index the thermal stability in terms of polyol
 235 composition. Ternary plot (Figure 4A) showed a red area with the increase of PCL and PE. Addition
 236 of PEG to the mixture reduce the nAUC. This is accorded with the behavior of onset temperature
 237 suggesting that higher values of nAUC represents higher thermal stability and lower values
 238 represents lower thermal stability of polyurethanes. ANOVA (Table 2) showed a linear model where
 239 the terms of each component were significant. Standardized coefficients showed that the influence of
 240 composition follow PE>PCL>PEG.

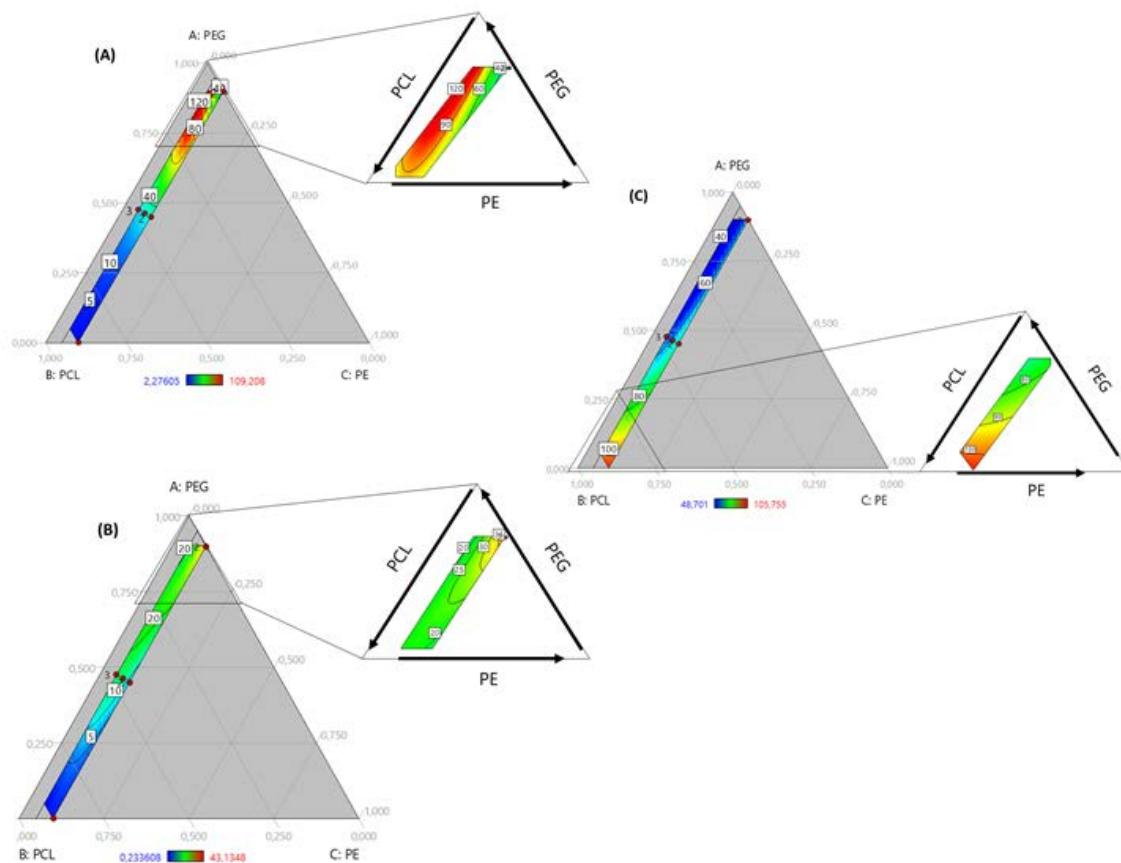
241 2.4. Hydrophilicity and hydrolytic degradation

242 To evaluate the hydrophilicity, water absorption and water contact angle were evaluated. Figure
 243 2A shows the contour plot of water absorption (non-transformed). There is an increased swelling
 244 with an increase in the PEG fraction. Conversely, swelling decreased with the amount of PCL. PEG
 245 and PCL are hydrophilic and hydrophobic polyols, respectively. These responses indicated that the
 246 nature of the polyols regulated the swelling response. Despite the urethane bonds, polyurethane
 247 chains conserve the structure of polyols, influencing the polyurethane response. Here, we observed
 248 how the incorporation of PEG increased the water absorption to levels that were approximately 30%
 249 due to the hydrophilic nature, and the largest amount of PCL showed the lowest swelling.

250 Likewise, an increase in the PE fraction involved a reduction in swelling. PE added to the hard
 251 segment and increased the crosslinking of the chains, causing a reduction on chains mobility[2]. In
 252 Figure 2A, we observe that increasing PE reduced the red area, or swelling, while a lower amount of
 253 PE showed a higher percentage of water absorption. According with Shoaib et al. (2018), a higher
 254 value of water absorption indicated an amorphous nature and decreased intermolecular density. In
 255 PUs, the hard segments acted as a twisting path for the diffusion of water molecules and the
 256

257 absorption increased with an increase in chain flexibility, providing more space for water molecules
 258 [6].

259
 260 Checking the ANOVA results (see Table 1), the triple interaction (PEG*PCL*PE) was significant and
 261 confirmed by the standard regression coefficients, in which the triple interaction coefficient was the
 262 highest between the significant terms ($\beta = 7.65$). That is consistent with the analysis of the ternary plot
 263 (Figure 3A), concluding that the bulk composition of polyurethanes regulated the water absorption.



264

265 Figure 3. Ternary contour plots of (A) Water absorption, (B) Hydrolytic degradation, (C) Contact
 266 angle. Red dots are design points, arrows indicated the increasing of each component.

267
 268 Contact angle measures the affinity between the solvent and material surface. Here, water was used
 269 as a solvent; therefore, wettability was evaluated. Lower angles indicate enhanced wettability. The
 270 surface is considered hydrophobic when contact angles are over 90° [16]. In Figure 3B, we can observe
 271 a decrease in the contact angle with an increase in the PEG content. The hydrophilic nature of PEG
 272 improved the interaction between water and PUs. Conversely, a rise in PCL increased the angle due
 273 to hydrophobic character of the polyol. PCL concentrations over 75% produced hydrophobic
 274 surfaces. However, this property did not change with the PE concentration. According to the ANOVA
 275 of regression model (Table 1. ANOVA test of model regression for water absorption, contact angle
 276 and hydrolytic degradation), there is a significant effect for PEG*PCL interaction. This interaction
 277 had a negative impact on response, agreeing with the standard regression coefficients ($\beta = -61.04$)
 278 producing polymers with lower contact angle. Water contact angle is a surface property, and the
 279 model suggests that the soft segments of PUs regulate this property.

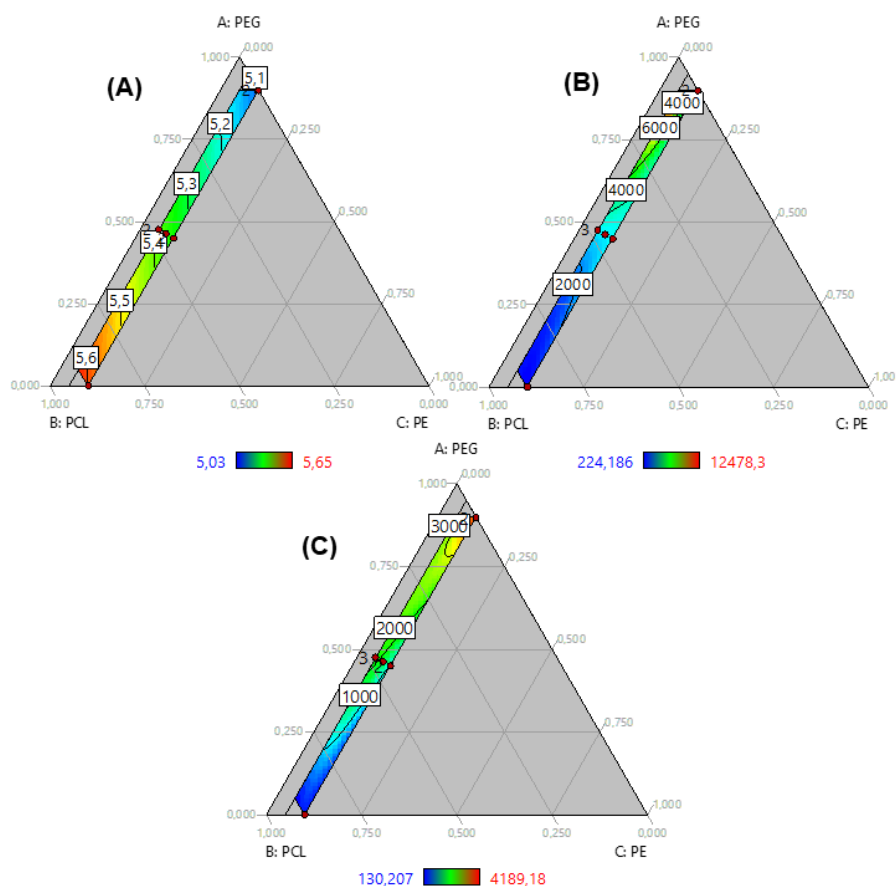
280

281 Hydrolytic degradation occurred after swelling. Water enters the PU matrix. Chain scission takes
 282 place through hydrolysis, in which water molecules may facilitate the cleavage of some bonds such
 283 as urethane and esters [17]. As mentioned previously, this property is related to the swelling of water
 284 and hydrophilicity [18]. Thus, in Figure 3C, the largest amount of PCL had the lowest weight loss.

285 Yet, increasing PEG content represents an increase in degradation. Hydrophilicity increased with
286 contact angle, and a rise in water uptake resulted in an enhancement of degradation. However, there
287 is a yellow to red area with the growth of PE at highest PEG concentrations. The addition of
288 crosslinkers increased the urethane bond content, which has a hydrolysable ester bond. Furthermore,
289 PEG is hydrolysable and produces carboxylic and hydroxyl groups on its surface, making it highly
290 hydrophilic and increasing the rate of degradation[6]. This suggests that swelling and hard segment
291 content synergistically enhance degradation. As such, the lowest degradation rate occurred with
292 higher concentrations of PCL, where the swelling is reduced. Model regression ANOVA showed that
293 the triple effect (Table 1) was significant. It suggested that three components regulate degradation.
294 As with water absorption, hydrolytic degradation is another bulk property that is directly regulated
295 by its composition.

296
297 To observe the behavior of water absorption and hydrolytic degradation with time. Area under
298 the curve was calculated for each sample. The effect of polyol blend composition on kinetics was
299 studied by a model regression. Our findings confirm the behavior described for water absorption and
300 hydrolytic degradation for 48h. In the first case (See Figure 4B) PUs with large swelling had largest
301 area under the curve. In ternary plot there is a red area at greater values of PEG and lower of PE like
302 Figure (WA). In the case of hydrolytic degradation described behavior like hydrolytic degradation at
303 48h (See Figure 4C). Lowest values of area under the curve relates with lowest weight loss. ANOVA
304 (Table 2) shows that triple interaction is significant for both responses. Triple interaction had a
305 negative influence in water absorption kinetics while have positive effect on degradation kinetics.

306
307 Finally, measurement of area under the curve of those kinetics could be understood as the hydrolytic
308 stability of PUs and. Higher values of area under of water absorption kinetics are related with largest
309 values area under the curve of degradation kinetics indicating that PUs are affected by hydrolytic
310 degradation.

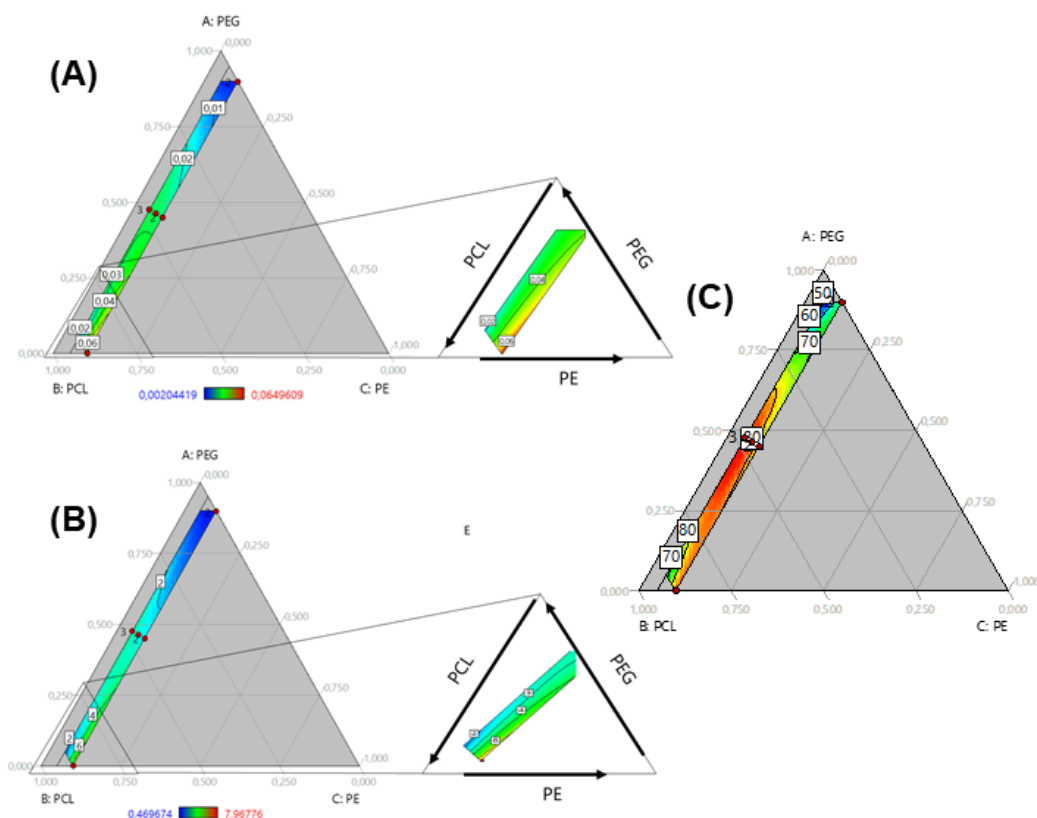


311
 312 Figure 4. Ternary contour plot of (A) thermal stability, (B) Water absorption kinetics and (C)
 313 hydrolytic degradation kinetics

314 2.5. Mechanical properties

315 The mechanical performance of PUs can be regulated by hard segment content or polyol
 316 characteristics, such as molecular weight and hydroxyl index. In Figure 5A, tensile strength and
 317 modulus are presented. In both cases, properties rise with the amount of PCL and PE. As mentioned
 318 previously, PE increases the hard segment content in PUs, modulating mechanical response. The hard
 319 segment interacts through hydrogen bonds, generating crosslinking[19], and a reduction in chain
 320 movement could enhance mechanical performance. Increasing the PE concentration promoted
 321 urethane linkage formation. Additionally, PE functionality of 4 allowed for the formation of a
 322 branched structure. It can reticulate the structure and increase crosslinking. PE influence can be
 323 observed by the standard regression coefficient, $\beta=102.12$ and $\beta=0.19$ for tensile strength and
 324 modulus, respectively. Despite this, the hydroxyl index was higher for PEG, suggesting that the
 325 molecular weight of the monomer can regulate mechanical behavior as well. In Figure 5B, modulus
 326 is improved by PCL addition. Here, the molecular weight of PCL was greater than that of PEG,
 327 creating larger chains and increasing the crosslinking.

328
 329 Additionally, model regression ANOVA showed a significant triple interaction (Table 3), suggesting
 330 that both mechanical properties are mediated by all three components



331

332 Figure 5. Ternary contour plots of (A) Tensile stretch and (B) Modulus as function of PEG, PCL and
 333 PE mass fraction

334 Hardness of PUs was evaluated too. Increase of PE concentration represent a rise of hardness and
 335 largest values was reached at high concentration of PCL (Figure 5C). ANOVA (See Table 3) showed
 336 significant triple interaction with a positive influence, according with standardized coefficients. Our
 337 results suggest that, in addition to crosslinking, the molecular weight of polyols mediated in
 338 mechanical properties.

339

340 Regression of elongation at break was carried out, but it showed low fitting properties (R-square
 341 =0.35). This property was not analyzed in this work.

342 2.6. Model Validation

343 Our models were validated by the check point method (See Table 7). The response of check
 344 materials in properties like water absorption, hydrolytic degradation, tensile strength and contact
 345 angle was carried out in Design Expert 10 based on the confidence intervals at 95%. The response of
 346 the materials adjusts to the model's responses. It suggests that our models can predict the structure
 347 properties relationship of polyurethanes based on the composition of the polyol blend and can be
 348 used to navigate the design space and optimize desired properties.

349 4. Materials and Methods

350 4.1. Materials

351 The following reagents were used for PUs synthesis: polycaprolactone diol (PCL) with average
 352 molecular weight of $M_n \sim 2000$, isophorone diisocyanate (IPDI), N,N-dimethylformamide (DMF) were
 353 purchased from Sigma-Aldrich, USA. Polyethylene glycol (PEG, $M_n \sim 1000$) was from Merck KGaA,

354 Germany, and pentaerythritol (PE) was from Alfa Aesar, England. For characterization analysis,
355 phosphate buffer saline (PBS) was purchased from VWR, USA.

356 4.2. Polyurethane synthesis

357 Polyurethanes were synthesized via a two-step polymerization. PCL and PEG were used as
358 polyols, PE and IPDI as crosslinkers and NCO as a source, respectively.

359 Each weighted polyol was preheated at 110°C and mixed with 10 ml of DMF, and then IPDI, in a
360 NCO/OH ratio of 1, was added and allowed to react for 15 min at 70°C with agitation. In parallel, PE
361 was diluted in 10 mL of DMF at 110°C with agitation. Next, the PE solution was added to the
362 prepolymer. A vacuum was applied to remove air. Finally, each polymer was poured in cylindrical
363 molds and cured at 110°C for 12 hours. After the curing period, PUs were washed in a 50% (v/v)
364 ethanol-water solution for 1 hour to remove mold, released and dried at 80°C.
365

366 4.3. Design of experiment

367 In this work, the effect of the polyol blend composition on several properties of polyurethanes was
368 studied through mixture design. PCL, PEG and PE composition, in mass fraction, was varied in the
369 ranges shown in **Table 1**

370 **Table 6:** Variation ranges in experimental design for polyurethanes synthesis

Blend Component	Lower Limit*	Upper Limit*
PEG	0.000	0.900
PCL	0.000	0.900
PE	0.050	0.100

371 *Mass fraction

372 A special cubic model was used to study linear, double and triple effects and the sum of
373 composition must be one. **Table 7** describes the blend and point type, as well as the composition of
374 each material. Each property studied was measured three times, and the average value was used for
375 the model regression. Data analysis and model regression were carried out in Design Expert V10.

376 Before regression, outliers and influential point were evaluated by Cook's distance and DFFITS test.
377 Box-Cox distribution was evaluated, and recommended transformation was applied. Model
378 regression was made by minimum least squares. Analysis of variance (ANOVA) was carried out for
379 model validation and the evaluation of significant terms.

380

381

382

383

384 **Table 7.** Description of mixture design for the study of polyol blend composition

Blend	Type	Sample Name	PEG*	PCL*	PE*
Binary	Vertex	S1	0.000	0.900	0.100
Binary	Vertex	S2	0.000	0.900	0.100
All components	Edge centroid	S3	0.025	0.900	0.075
All components	Vertex	S4	0.050	0.900	0.050

All components	Vertex	S5	0.050	0.900	0.050
All components	Edge centroid	S6	0.450	0.450	0.100
All components	Edge centroid	S7	0.450	0.450	0.100
All components	Edge centroid	S8	0.450	0.450	0.100
All components	Overall centroid	S9	0.463	0.463	0.075
All components	Edge centroid	S10	0.475	0.475	0.050
All components	Edge centroid	S11	0.475	0.475	0.050
Binary	Vertex	S12	0.900	0.000	0.100
Binary	Vertex	S13	0.900	0.000	0.100
Binary	Vertex	S14	0.900	0.000	0.100
All components	Edge centroid	S15	0.900	0.025	0.075
All components	Vertex	S16	0.900	0.050	0.050
Check Point		C1	0.571	0.33	0.099
Check Point		C2	0.815	0.091	0.094
Check Point		C3	0.796	0.107	0.097

385 *Mass fraction

386 4.4. Polyurethanes characterization

387 The chemical structure of PUs was evaluated by Fourier-transform infrared spectroscopy (FTIR)
 388 from a range of 400 cm⁻¹ to 4000 cm⁻¹ in a Nicolet iS10 (Thermo Scientific, USA). The experiment was
 389 setup in 32 scans and resolution of 4.

390
 391 Thermal behavior was studied by thermogravimetric assay in a TGA/DSC 1 (Mettler Toledo, USA).
 392 The method consisted of two steps. The first was at 105°C for 1 hour to remove water and solvent
 393 traces. The second a dynamic heating from 105 to 600°C at rate of 10°C/min. Tests were carried out
 394 under nitrogen atmosphere with a flow of 180 ml/min. Curve were normalized respect to initial
 395 weight of the sample. DTGs, onset temperatures and normalized area under de curve were calculated
 396 using the STARe software provided by the TGA/DSC1 supplier.

397
 398 Contact angle was determined using a MobileDrop (KRÜSS GmbH, Germany) with distilled water
 399 at room temperature and the sessile drop method. At least 3 measurements per polymer were taken,
 400 and the average of those was reported.

401
 402 Water absorption was evaluated by soaking each sample in triplicate in 1 ml of PBS 1x. Samples were
 403 incubated for 48 hours at 37°C. Swelling was calculated with the initial weight (Wo) and the final
 404 weight (Ws), according with the following equation:

$$405 \quad \% \text{Water absorption} = (W_s - W_o) / W_o, \quad (1)$$

406
 407 Hydrolytic degradation was analyzed by soaking the samples in PBS 1x as before. After 48 hours,
 408 samples were dried in an oven at 80°C until a constant weight was reached. The dried weight was
 409 recorded (Wi), and degradation was calculated as follows:

$$410 \quad \% \text{Degradation} = (W_o - W_i) / W_o, \quad (2)$$

411
 412 Kinetics of water absorption and hydrolytic degradation were carried out, following the method
 413 described for each property. At least 5 time points were recorded in interval of 120 hours. Curve were
 414 analyzed based on the %Water absorption and %Degradation. Under the curve area was calculated
 415 using the trapezoid method.

416

417 The mechanical properties of PUs were assessed by uniaxial tensile test with EZ-XL universal test
418 machine (Shimadzu, Japan) at 10 mm/min. Ultimate stress, modulus and elongation at break were
419 recorded. Shore A hardness was measured using a shore A durometer. 10 measurements were
420 recorded for each sample and the average was used for the model regression.

421 5. Conclusions

422 Application of the mixture design allowed for us to set mathematic relationships for the effects
423 of polyol blend composition on properties of polyurethane obtained from PEG and PCL (polyols), PE
424 (crosslinker) and IPDI (isocyanate). An ANOVA test and fit statistics suggested a good fit and
425 predictive potential with those equations.

426
427 Water absorption, hydrolytic degradation and contact angle responses were regulated by the polar
428 nature of polyols and crosslinker concentrations. However, tensile strength, modulus and hardness
429 could be mediated by other characteristics of polyols such as molecular weight and hydroxyl value,
430 together with the crosslinker concentration. From a statistical perspective, a triple interaction
431 (PEG*PCL*PE) with water absorption, hydrolytic degradation, tensile strength, hardness and
432 modulus was significant, but not for contact angle, where the PEG*PCL interaction was significant.
433 This suggests that bulk properties such as those in the first group are regulated by three components
434 composition, but contact angle, as a surface property, is mediated by the polyol nature. Thermal
435 stability was evaluated by area under the curve of the DTGs. It shows that increase of PCL and PE
436 improved stability. Additionally, hydrolytic stability was evaluated by area under the curve from the
437 water absorption and hydrolytic degradation kinetics where similar behavior was observed. Showing
438 that are under the curve could be used to transform curve identifying effects of variables.

439
440 To conclude, this methodology allowed for a better understanding of the structure-property
441 relationship through a mathematic model, identifying the main effects of the polyol blend
442 composition on the final properties. These models look promising for optimization to design a
443 polyurethane with target properties, and the mixture design could extrapolate to other components
444 such as isocyanate and the NCO/OH ratio.

445 **Author Contributions:** Conceptualization, Said Arévalo-Alquichire, Manuel Valero and Luis Diaz.;
446 Methodology, Said Arévalo-Alquichire and Maria Morales-Gonzalez; Software, Said Arévalo-Alquichire.;
447 Validation, Said Arévalo-Alquichire; Formal Analysis, Said Arévalo-Alquichire; Investigation, Said Arévalo-
448 Alquichire and Maria Morales-Gonzalez.; Resources, Manuel Valero; Writing-Original Draft Preparation, Said
449 Arévalo-Alquichire; Visualization, Said Arévalo-Alquichire; Supervision, Manuel Valero and Luis Diaz; Project
450 Administration, Manuel Valero; Funding Acquisition, Manuel Valero

451 **Funding:** This research was funded by Universidad de La Sabana under grant ING-176-2016

452 **Acknowledgments:** The authors would like to thank to Dr. Maria Ximena Quintanilla for access to Design Expert
453 V.10. SAA thanks Dr. Edgar Benitez for advice regarding statistical analysis and experimental design and to the
454 department of science, technology and innovation COLCIENCIAS from Colombia for the funds for doctoral
455 training under the grant, 727-2015.

456 **Conflicts of Interest:** The authors declare no conflict of interest.

457

458 References

- 459 [1] S. Arévalo-Alquichire and M. Valero, "Castor Oil Polyurethanes as Biomaterials," in *Elastomers*, N.
460 Çankaya, Ed. Rijeka: InTech, 2017, pp. 137–157.
- 461 [2] P. Jutrzenka Trzebiatowska, A. Santamaria Echart, T. Calvo Correias, A. Eceiza, and J. Datta, "The
462 changes of crosslink density of polyurethanes synthesised with using recycled component. Chemical
463 structure and mechanical properties investigations," *Prog. Org. Coatings*, vol. 115, pp. 41–48, Feb. 2018.
- 464 [3] N. Nagiah, R. Johnson, R. Anderson, W. Elliott, and W. Tan, "Highly Compliant Vascular Grafts with

- 465 Gelatin-Sheathed Coaxially Structured Nanofibers," *Langmuir*, vol. 31, no. 47, pp. 12993–13002, Dec.
466 2015.
- 467 [4] M. Bil, J. Ryszkowska, P. Woźniak, K. J. Kurzydłowski, and M. Lewandowska-Szumieł, "Optimization
468 of the structure of polyurethanes for bone tissue engineering applications," *Acta Biomater.*, vol. 6, no. 7,
469 pp. 2501–2510, Jul. 2010.
- 470 [5] Y. L. Uscátegui, S. J. Arévalo-Alquichire, J. A. Gómez-Tejedor, A. Vallés-Lluch, L. E. Díaz, and M. F.
471 Valero, "Polyurethane-based bioadhesive synthesized from polyols derived from castor oil (*Ricinus*
472 *communis*) and low concentration of chitosan," *J. Mater. Res.*, vol. 32, no. 19, pp. 3699–3711, Oct. 2017.
- 473 [6] M. Shoaib, A. Bahadur, A. Saeed, M. S. ur Rahman, and M. M. Naseer, "Biocompatible, pH-responsive,
474 and biodegradable polyurethanes as smart anti-cancer drug delivery carriers," *React. Funct. Polym.*, vol.
475 127, pp. 153–160, Jun. 2018.
- 476 [7] L. Eriksson, E. Johansson, and C. Wikström, "Mixture design—design generation, PLS analysis, and
477 model usage," *Chemom. Intell. Lab. Syst.*, vol. 43, no. 1–2, pp. 1–24, Sep. 1998.
- 478 [8] M. A. Bezerra, R. E. Santelli, E. P. Oliveira, L. S. Villar, and L. A. Escalera, "Response surface
479 methodology (RSM) as a tool for optimization in analytical chemistry," *Talanta*, vol. 76, no. 5, pp. 965–
480 977, Sep. 2008.
- 481 [9] A. Khaskhoussi, L. Calabrese, H. Bouhamed, A. Kamoun, E. Proverbio, and J. Bouaziz, "Mixture design
482 approach to optimize the performance of TiO₂ modified zirconia/alumina sintered ceramics," *Mater.*
483 *Des.*, vol. 137, pp. 1–8, Jan. 2018.
- 484 [10] J. B. Olivato, M. M. Nobrega, C. M. O. Müller, M. A. Shirai, F. Yamashita, and M. V. E. Grossmann,
485 "Mixture design applied for the study of the tartaric acid effect on starch/polyester films," *Carbohydr.*
486 *Polym.*, vol. 92, no. 2, pp. 1705–1710, Feb. 2013.
- 487 [11] L. Abolghasemi Fakhri, B. Ghanbarzadeh, J. Dehghannya, F. Abbasi, and H. Ranjbar, "Optimization of
488 mechanical and color properties of polystyrene/nanoclay/nano ZnO based nanocomposite packaging
489 sheet using response surface methodology," *Food Packag. Shelf Life*, vol. 17, pp. 11–24, Sep. 2018.
- 490 [12] H. Li *et al.*, "Preparation and characterization of bio-polyol and bio-based flexible polyurethane foams
491 from fast pyrolysis of wheat straw," *Ind. Crops Prod.*, vol. 103, pp. 64–72, Sep. 2017.
- 492 [13] D. Zhao, G. Wang, and M. Wang, "Investigation of the effect of foaming process parameters on
493 expanded thermoplastic polyurethane bead foams properties using response surface methodology," *J.*
494 *Appl. Polym. Sci.*, vol. 135, no. 25, p. 46327, Jul. 2018.
- 495 [14] H. L. Sui, X. Y. Liu, F. C. Zhong, X. Y. Li, and X. Ju, "A study of radiation effects on polyester urethane
496 using two-dimensional correlation analysis based on thermogravimetric data," *Polym. Degrad. Stab.*, vol.
497 98, no. 1, pp. 255–260, Jan. 2013.
- 498 [15] P. Król and B. Pilch-Pitera, "Phase structure and thermal stability of crosslinked polyurethane
499 elastomers based on well-defined prepolymers," *J. Appl. Polym. Sci.*, vol. 104, no. 3, pp. 1464–1474, May
500 2007.
- 501 [16] N. L. Tai, R. Adhikari, R. Shanks, P. Halley, and B. Adhikari, "Flexible starch-polyurethane films: Effect
502 of mixed macrodiol polyurethane ionomers on physicochemical characteristics and hydrophobicity,"
503 *Carbohydr. Polym.*, vol. 197, pp. 312–325, Oct. 2018.
- 504 [17] S. Arévalo-Alquichire *et al.*, "Polyurethanes from modified castor oil and chitosan," *J. Elastomers Plast.*,
505 vol. 0, no. 0, p. 009524431772957, Sep. 2017.
- 506 [18] L. Romero-Azogil, E. Benito, A. Martínez de Ilarduya, M. G. García-Martín, and J. A. Galbis, "Hydrolytic
507 degradation of d -mannitol-based polyurethanes," *Polym. Degrad. Stab.*, vol. 153, pp. 262–271, Jul. 2018.

508 [19] M. F. Valero Valdivieso, "Degradación In-Vitro de Mezclas de Poliuretano Termoplástico Y Almidón
509 Modificado," *Polímeros Ciência e Tecnol.*, vol. 23, no. 3, pp. 373–382, 2013.
510

511 **Sample Availability:** Samples of the compounds are available from the authors.